Consequences of resonant impurity scattering in anisotropic superconductors: Thermal and spin relaxation properties

P. J. Hirschfeld* and P. Wölfle
Department of Physics, University of Florida, Gainesville, Florida 32611

D. Einzel
Walther-Meissner-Institut für Tieftemperaturforschung, D-8046 Garching, Federal Republic of Germany
(Received 25 June 1987)

We present a systematic discussion of the effect of resonant impurity scattering on anisotropic model states of heavy-fermion superconductors. The impurity scattering is treated in the self-consistent T-matrix approximation including a renormalization of the frequency ω and the quasiparticle energy ξ_k. Model states considered include the axial and polar states familiar from superfluid ^{3}He as well as two states, termed hexial and hybrid, occurring in the group-theoretical classification of singlet states in hexagonal symmetry. We calculate the density of states, the critical temperature and the order parameter, the specific heat, the thermal conductivity, and the spin-lattice relaxation rate. Vertex corrections are included in the calculations of two-particle quantities. The observed properties of the prototype Fermi-liquid material UPt_3 show many qualitative features in common with our model. However, it turns out to be difficult to identify any given state with certainty. An experimental test of our predictions on the behavior as a function of impurity concentration, particularly in the gapless regime at low temperatures, would allow for a more definitive characterization of the superconducting state.

I. INTRODUCTION

There now exists a considerable body of data[1] on the thermodynamic and transport properties of the three currently known "heavy-fermion" superconductors $CeCu_2Si_2$, UBe_{13}, and UPt_3, against which theories of the superconducting state in these compounds must be tested. All measurements to date deviate strongly from the predictions of the BCS (weak-coupling) theory, otherwise so successful in describing many aspects of "ordinary" superconductivity in less strongly interacting systems. A number of authors[2-5] have suggested that an extremely anisotropic order parameter could be responsible for the anomalous temperature dependences observed in experiments on heavy-fermion systems. The best known example of this type of order is the well-studied superfluid A phase of ^{3}He, where the order parameter actually vanishes at points on the Fermi surface. The existence of Bogoliubov quasiparticle excitations in the neighborhood of these nodes gives rise to a non-BCS behavior in the specific heat $C(T)$ and other measured properties, particularly at low temperatures where the node contributions are dominant. Power laws in temperature predicted by the simplest version of BCS theory in the presence of such highly anisotropic correlations should depend, at the very lowest temperatures, only on the dimension of the manifold of gap nodes (i.e., points or lines) and the rate at which the gap vanishes in the neighborhood of the nodes.

The hypothesis of anisotropic pairing, while qualitatively successful in explaining specific-heat measurements,[2] has been shown to fail when applied to the calculation of transport coefficients in the Born approximation.[6] Simple estimates indicate that the product of the quasiparticle scattering time and density of states is essentially energy independent for all anisotropic gap structures, leading to transport coefficients with temperature dependencies identical to those in the normal state. (More precisely, in those cases where the transport coefficient is a tensor quantity, the largest eigenvalue behaves in this way.) This is in stark contrast to the temperature dependences actually observed in heavy-fermion superconductors, where power laws in temperature with exponent higher than that observed above the transition have been claimed.[2-5]

A resolution of this dilemma was proposed by Pethick and Pines,[7] who argued that nonmagnetic impurities in heavy-fermion systems give rise to an impurity potential which is strongly screened, such that the Friedel sum rule is essentially exhausted by the s-wave scattering phase shift $\delta_0 \simeq \pi q/N_f$. Here qe is the charge on the impurity and N_f the level degeneracy of the scattering electrons. In $CeCu_2Si_2$, crystal-field splitting is thought to result in a doublet ground state,[8] and there exists some evidence[9] that the same is true in the uranium compounds despite the complications of strong spin-orbit coupling. In this case a singly charged impurity gives rise to scattering in the unitary limit $\delta_0 \simeq \pi/2$ as suggested by Hirschfeld *et al.*,[10] hereafter referred to as I. In a complementary approach, Schmitt-Rink *et al.*[11] have suggested that a substitutional impurity or vacancy in a Kondo lattice is associated with a relative Kondo phase shift of $\pi/2$ with respect to the lattice background.

The consequences of the assumption of resonant scattering are important in both the normal and superconducting states. Pethick and Pines[7] showed that the dramatically enhanced transport relaxation rates exhibit-

ed by the three heavy-fermion superconductors at low temperatures could be qualitatively understood on this basis. The conclusion follows essentially from the variation of the quasiparticle relaxation rate $1/\tau$ in the unitary limit with $N(\omega)/[G'(\omega)]^2$, where $G'(\omega)\sim\omega$ over a wide intermediate frequency range (G' is the real part of the single-particle propagator). Consideration of the calculated frequency dependence of $1/\tau$ for model anisotropic states then led Pethick and Pines to predictions for the temperature dependence of the longitudinal sound absorption and thermal conductivity at variance with at least some of the experimental results on UBe_{13} and UPt_3. Subsequently, Hirschfeld *et al.*[10] demonstrated that an analysis based on the leading-order frequency dependence of the density of states and similar quantities is not sufficient to make realistic predictions for the temperature dependencies of transport quantities in the anisotropic superconducting state. At very low temperatures, they showed that a self-consistent treatment of the resonant scattering leads to an unusual "gapless" behavior in which the system responds, even in the presence of very small impurity concentrations, much as in the normal state, albeit with a much reduced density of states. Closer to T_c, the temperature dependence of the order parameter combines with the upper cutoff in the frequency power laws to destroy the temperature power laws expected. Numerical results for the temperature-dependent specific heat, thermal conductivity, and ultrasound attenuation near the unitarity limit were compared in I with the available data for UPt_3 and found to be consistent with a line or possibly points of nodes in the hexagonal basal plane, given an impurity concentration of 10^{-3}–10^{-4} in nominally pure samples. Similar conclusions were reached by Schmitt-Rink *et al.*[11] and Scharnberg *et al.*[12]

Resonant impurity scattering can have equally important consequences for transport quantities in the heavy-fermion normal state. Varma[13] and Batlogg *et al.*[14] have emphasized the remarkable fact that mean free paths deduced from transport experiments on heavy-fermion compounds are of the same order of magnitude as in ordinary metals. Since the Fermi velocity scales inversely with the effective mass m^*, the relaxation time must vary as m^*. This may be explained by assuming a heavy-fermion self-energy $\Sigma(k,\omega)$ due to inelastic processes with negligible momentum dependence, as proposed by Varma, or in those cases where impurity scattering dominates, by assuming the existence of nearly resonant scatterers in the samples. In the latter case one also finds that τ varies as $N(\omega)\propto m^*$ in the normal state, just as in the superconductor.

In this work, we further explore the consequences of the resonant scattering assumption for the properties of heavy-fermion superconductors. In Sec. II, we present a more detailed account of the self-consistent T-matrix approximation for the impurity self-energy described in I. In Sec. III, we calculate various thermodynamic and transport properties for model order parameters with points and lines of nodes on the Fermi surface, as well as states allowed in hexagonal crystal symmetry under group-theoretical classifications,[15–18] and compare our results with the available experimental data on UPt_3. In addition to those properties discussed in I, we present new calculations of the nuclear magnetic relaxation rate $1/T_1$. The treatment of transport properties described in I is supplemented here by the addition of vertex corrections, which may be important even in the case of purely s-wave scatterers,[12] in contrast to the familiar results for isotropic superconductors.[19] A self-consistent T-matrix description of impurity-limited transport is shown to require renormalization of single-particle energies even in particle-hole symmetric systems, again in contrast to the isotropic case. We find, as expected, that various allowed states give results qualitatively similar to the model states considered in Sec. III. In particular, the results for the disallowed "polar" state, with an equatorial line of nodes on the Fermi surface, are mimicked by certain allowed anisotropic singlet states. Finally, in Sec. IV we present our conclusions and suggestions for further experimental and theoretical work.

In what follows we have concentrated primarily on comparisons of theory with data currently available for UPt_3. The other two heavy-fermion superconductors, $CeCu_2Si_2$, and UBe_{13}, are certainly not less interesting, and our neglect requires some justification. At present one major goal of our analysis is to rule out, if possible, all anisotropic states incompatible with experiment (in the framework of the anisotropic pairing hypothesis). Measurements of anisotropic thermal conductivity and ultrasound attenuation, which may prove particularly important tools in this effort, have at this writing been performed more exhaustively on UPt_3 than on the other two compounds. Perhaps more importantly, it is only in UPt_3 that we have, in the smallness of the specific-heat jump at the superconducting transition and the onset of coherence displayed in the low-temperature normal-state resistivity, strong indications that the system has entered a Fermi-liquid–like phase before it makes the transition to the superconducting state. Incorporation of resonant scattering effects into an anisotropic version of weak-coupling BCS theory may therefore be justified in UPt_3, since normal-state quantities may be taken as constant in energy on a scale of T_c. This does not appear to be the case in the two Kondo-lattice compounds $CeCu_2Si_2$ and UBe_{13}, where strong-coupling corrections are explicitly reflected in the large specific-heat jumps (see, however, experiments on UBe_{13} under pressure).[20] Nevertheless, there is no particular reason to assume that strong-coupling effects make as important a contribution to transport coefficients as they do to the one-particle properties. Varma[13] has, in fact, argued that they may vanish altogether. The results given below may, therefore, be in some cases relevant to $CeCu_2Si_2$ and UBe_{13} as well as UPt_3. In Sec. IV we discuss some interesting aspects of this comparison.

Because its calculation is considerably more involved than the other transport properties we consider here, we have considered the problem of hydrodynamic sound attenuation in anisotropic systems in a separate, complementary publication.[21] The calculation follows the method outlined here in Appendix B.

II. T-MATRIX APPROXIMATION FOR THE SELF-ENERGY

We consider the effect of potential scattering by spinless, noninteracting impurities on the single-particle propagator $\underline{g}(\mathbf{k},\omega)$ for superconducting electrons, which obeys the Dyson equation

$$[\omega\underline{\tau}^0-\xi_{\mathbf{k}}\underline{\tau}^3-\underline{\Delta}_{\mathbf{k}}-\underline{\Sigma}(\mathbf{k},\omega)]\underline{g}(\mathbf{k},\omega)=\underline{\tau}^0 . \tag{2.1}$$

Here $\xi_{\mathbf{k}}$ is the quasiparticle energy, $\underline{\Delta}_{\mathbf{k}}$ is the order parameter, $\underline{\tau}^j$ $(j=1,2,3)$ are the Pauli matrices, $\underline{\tau}^0$ is the unit matrix, and all underlined quantities represent matrices in particle-hole (Nambu) space. We suppress spin indices, which do not play a role in our discussion. The self-energy $\underline{\Sigma}(\mathbf{k},\omega)$ in a single-site approximation is

$$\underline{\Sigma}(\mathbf{k},\omega)=\Gamma\underline{T}(\mathbf{k},\mathbf{k},\omega) , \tag{2.2}$$

where $\Gamma=(n_i/\pi N_0)(N/V)$, n_i is the impurity concentration, N/V is the electron density, N_0 is the density of states, and $\underline{T}$ obeys the Lippmann-Schwinger equation

$$\underline{T}(\mathbf{k},\mathbf{k}',\omega)=\underline{V}(\mathbf{k},\mathbf{k}')+\sum_{\mathbf{k}''}\underline{V}(\mathbf{k},\mathbf{k}'')\underline{g}(\mathbf{k}'',\omega)\underline{T}(\mathbf{k}'',\mathbf{k}',\omega) . \tag{2.3}$$

Here $\underline{V}$ is the scattering potential for a single electron. It is convenient to rewrite (2.2) in terms of the normal state ($\Delta_k=0$) K matrix, which contains the details of the complicated scattering problem in the normal state. We therefore split off the off-shell part of the normal-state propagator g'_N, and resume:

$$\underline{T}=\underline{V}+\underline{V}(\underline{g}-\underline{g}'_N+\underline{g}'_N)\underline{T} \tag{2.4a}$$

$$=(\underline{V}+\underline{V}\underline{g}'_N\underline{V}+\underline{V}\,\underline{g}'_N\underline{V}\underline{g}'_N\underline{V}+\cdots)[\underline{1}+(\underline{g}-\underline{g}'_N)\underline{T}] \tag{2.4b}$$

$$\equiv\underline{K}_N+\underline{K}_N(\underline{g}-\underline{g}'_N)\underline{T} . \tag{2.4c}$$

We now exploit the fact that $\underline{K}_N$ and, by extension, $\underline{T}$ vary slowly in energy with respect to the sharply peaked on-shell part of the Green's function; the off-shell part g' tends to its normal-state value for energies outside a shell of width Δ about the Fermi energy. This collapses the energy part of the momentum sum in (2.4c). If we further assume that the scattering potential is strongly screened, the angular dependence of $\underline{K}_N$ and $\underline{T}$ over the Fermi surface may be neglected, and we arrive at

$$\underline{T}(\omega)=\underline{K}_N+\underline{K}_N\sum_{\mathbf{k}}[g(\mathbf{k},\omega)-g'_N(\mathbf{k},\omega)]\underline{T}(\omega) , \tag{2.5}$$

where we have explicitly neglected the frequency dependence of the normal state K matrix, since K_N varies on an energy scale $E_F\gg T_c$. The principal-part integration $\sum_{\mathbf{k}}g'_N$ vanishes, leaving us with

$$\underline{T}(\omega)=\underline{K}_N+\underline{K}_N\underline{G}(\omega)\underline{T}(\omega) , \tag{2.6}$$

where $\underline{G}(\omega)\equiv(1/\pi N_0)\sum_{\mathbf{k}}\underline{g}(\mathbf{k},\omega)$, and N_0 is the density of states at the Fermi surface. With the usual parametrization of the K matrix in terms of an s-wave scattering phase shift δ_0, $K_N\equiv-\tan\delta_0$, Eqs. (2.1), (2.2), and (2.6) now allow for the straightforward calculation of the single-particle propagator in the presence of impurities of arbitrary concentration and scattering strength.

We proceed to a solution by expanding all matrix quantities as $\underline{\Sigma}=\sum_{j=0}^{3}\Sigma_j\underline{\tau}^j$. The formal expression for the one-particle Green's function is then

$$\underline{g}(\mathbf{k},\omega)=\frac{1}{\tilde{\omega}^2-\tilde{\Delta}^2-\tilde{\xi}^2}(\tilde{\omega}\tau^0+\underline{\tilde{\Delta}}_{\mathbf{k}}+\tilde{\xi}_{\mathbf{k}}\underline{\tau}^3) , \tag{2.7}$$

where

$$\tilde{\omega}=\omega-\Sigma_0 , \tag{2.8a}$$

$$\tilde{\xi}_{\mathbf{k}}=\xi_{\mathbf{k}}+\Sigma_3 , \tag{2.8b}$$

$$\underline{\tilde{\Delta}}_{\mathbf{k}}=\underline{\Delta}_{\mathbf{k}}+\underline{\Sigma}_{12} , \tag{2.8c}$$

and $\underline{\Sigma}_{12}=\Sigma_1\underline{\tau}^1+\Sigma_2\underline{\tau}^2$. The general expressions for the solutions T_j to (2.6) are quite complicated and contain all components of the integrated Green's function G_j. A considerable simplification of the problem arises if one assumes (a) particle-hole symmetry, and (b) an order parameter odd under inversion (odd parity) *or* under another symmetry of the crystal (certain even-parity states also included). In this case the components $G_1=G_2=G_3=0$, and one need only calculate

$$G_0\equiv-i\left\langle\frac{\tilde{\omega}}{(\tilde{\omega}^2-\Delta_k^2)^{1/2}}\right\rangle_{\hat{\mathbf{k}}} \tag{2.9}$$

in order to obtain a consistent solution to (2.1), (2.2), (2.6), and the gap equation

$$\Delta_{\mathbf{k}}=-T\sum_{\omega_n}\sum_{\mathbf{k}'}V_{\mathbf{k}\mathbf{k}'}\tfrac{1}{2}\mathrm{Tr}[(\underline{\tau}^1+\underline{\tau}^2)g(\mathbf{k}',\omega_n)] , \tag{2.10}$$

where $V_{\mathbf{k}\mathbf{k}'}$ is the pair potential. In (2.9) the angular brackets denote an average over solid angle. It is not immediately obvious that the quantities

$$G_3\equiv\frac{1}{\pi N_0}\sum_{\mathbf{k}}\frac{\tilde{\xi}}{\tilde{\omega}^2-\tilde{\xi}^2-\tilde{\Delta}_k^2}$$

and (2.11)

$$\underline{G}_{12}\equiv\frac{1}{\pi N_0}\sum_{\mathbf{k}}\frac{\underline{\tilde{\Delta}}_k}{\tilde{\omega}^2-\tilde{\xi}^2-\tilde{\Delta}_k^2}$$

may be taken to vanish even if the single-particle spectrum and pair function of the pure system manifest the symmetries (a) and (b) above. That this is indeed the case is shown in Appendix A. Then $\underline{T}$ takes on the particularly simple form $\underline{T}=T_0\underline{\tau}^0+T_3\underline{\tau}^3$, where

$$T_0=\frac{G_0}{c^2-G_0^2},\quad T_3=\frac{-c}{c^2-G_0^2} , \tag{2.12}$$

and $c\equiv\cot\delta_0$ is a convenient measure of the scattering strength, with $c=0$ in the unitary limit and $c\gg1$ for weak scattering. Furthermore, only T_0 is necessary for the calculation of single-particle properties via (2.7) and (2.8a). On the other hand, the full structure of the T matrix must be included in all two-particle correlation functions. As a practical matter, this means that the single-particle energies in g must be renormalized as in (2.8b). This complication does not arise in the usual Abrikosov-Gor'kov theory of impurity scattering in the Born approximation, since $\Sigma_3^{\mathrm{Born}}=\mathrm{const}$ under the usual particle-hole symmetry assumption, and may be absorbed into the chemical potential. The effect of Σ_3 in

this case thus vanishes in both the weak- and strong-scattering limits, since from (2.12) $\Sigma_3 \to 0$ as $c \to 0$. The results of I, which neglected this renormalization even for finite c, are nonetheless essentially unchanged near the unitarity limit, as shown in Sec. III.

If deviations from the resonant scattering limit are small, inclusion of Σ_3 in G is qualitatively important only for these superconducting two-particle properties for which vertex corrections due to impurity scattering play an essential role. In particular, the consistent treatment of Σ_3 eliminates an unphysical singularity in the collision contribution to the longitudinal sound attenuation.[21] Thus the treatment of Scharnberg *et al.*[12] is inconsistent except in the unitary limit. An improved version of their theory has recently been put forward.[23]

If $c \simeq 1$, qualitative changes in transport coefficients may be expected, particularly with regard to anisotropy. For example, off-diagonal components of the thermal conductivity for uniaxial states arise through the self-consistent treatment of vertex corrections and Σ_3. As c is thought to be small compared to one in heavy fermion systems, we do not treat these effects here.

III. THERMODYNAMIC AND TRANSPORT PROPERTIES FOR MODEL ANISOTROPIC STATES

In a pure anisotropic superconductor, thermodynamic and transport properties are characterized at the lowest temperatures by power laws $(T/T_c)^\kappa$ if the gap vanishes somewhere on the Fermi surface. This is because thermally excited Bogoliubov quasiparticles may exist in the neighborhood of the gap nodes even at the lowest temperatures, in contrast to the usual BCS case, where excitations may be created over the finite gap only with probability $e^{-\Delta/k_B T}$. In the Born approximation, small concentrations of impurities are known to preserve the power laws, albeit with modified prefactors, for states with point nodes, while destroying those for states with lines of nodes. For sufficiently large concentrations, typically $\Gamma^{\rm Born} \sim \Delta_0$, zero-energy single-particle excitations are present for any type of state. If one considers the density of angle-resolved single-particle excitations

$$N_{\hat{\mathbf{k}}}(\omega) \equiv -(1/\pi)\,\mathrm{Im}\int d\xi\, g(\mathbf{k},\omega)\ ,$$

one sees that what happens is that the nodes of the energy gap $\Omega_G(\hat{\mathbf{k}})$ are broadened to include small *areas* of the Fermi surface. This gives rise to thermodynamic and transport properties similar to the normal state, albeit with a much reduced density of states. The importance of the unitarity limit in this regard is that scattering is much more rapid, and therefore that part of the Fermi surface "goes normal" at significantly smaller impurity concentration. We will refer to behavior of this type as "gapless," since similar effects are observed in ordinary dirty superconductors when the gap vanishes completely. A common confusion in the current literature arises because of the further use of the term "gapless" to mean a system with finite density of states at all energies, a characterization which may apply to anisotropic superconductors even without impurities.

A. Gap anisotropy

The simplest possible model states displaying nodes in the order parameter $\Delta_{\mathbf{k}}$ are the polar and axial solutions to the gap equation (2.10) for a pure $L=1$ pair potential, with angular structures $\Delta_{\mathbf{k}} = \Delta_0 \cos\theta_{\hat{\mathbf{k}}}$ and $\Delta_{\mathbf{k}} = \Delta_0 \sin\theta_{\hat{\mathbf{k}}}$, respectively. It has become commonplace in discussions of anisotropic superconductivity to present results for these two states, since many order parameters consistent with the crystal symmetry of the heavy-fermion compounds display similar lines or points of nodes on the Fermi surface. If a quantitative comparison of theory with experiment is at all possible, however, more realistic states must be considered. In what follows we first discuss results for polar and axial states oriented with symmetry axis $\hat{\mathbf{l}}$ parallel to the hexagonal c axis, thereby duplicating to some extent results already given in I. Comparison with transverse sound-attenuation data in that work strongly indicated the presence of a line or points of nodes in the basal plane of the crystal. We therefore further discuss results for various states consistent with hexagonal symmetry[17–18] which fit this criterion. These include, firstly, a state already mentioned in I as a promising candidate, with a line of nodes in the plane and point nodes at the poles of the Fermi surface:

$$\Delta_{\mathbf{k}} = \Delta_0 \hat{\mathbf{k}}_z (\hat{\mathbf{k}}_x + i\hat{\mathbf{k}}_y)\ . \tag{3.1}$$

This state corresponds to the two-dimensional representation E_1 in the Volovik and Gor'kov[17] classification. For want of a better name, we refer to this d-wave state as "hybrid," since it displays axial and polarlike behavior. Secondly, we consider the "hexial" state, transforming according to the representation H_3^-, with six point nodes in the basal plane:[18]

$$\Delta_{\mathbf{k}} = \Delta_1[\hat{\mathbf{k}}_y(\hat{\mathbf{k}}_y^2 - 3\hat{\mathbf{k}}_x^2)\hat{\mathbf{z}}] + \Delta_2\{\hat{\mathbf{k}}_z[(\hat{\mathbf{k}}_x^2 - \hat{\mathbf{k}}_y^2)\hat{\mathbf{x}} - 2\hat{\mathbf{k}}_x\hat{\mathbf{k}}_y\hat{\mathbf{y}}]\}\ , \tag{3.2}$$

where $\hat{\mathbf{x}}$, $\hat{\mathbf{y}}$, and $\hat{\mathbf{z}}$ are spin directions. Here the ratio Δ_1/Δ_2 is not fixed by symmetry considerations, but must be determined from knowledge of the details of the pair potential.[15] All states considered, including those of even parity, are odd under some operation of the symmetry group of the crystal. Thus, as discussed in Sec. II, impurities do not renormalize the order parameter $\Delta_{\mathbf{k}}$, except through an overall reduction in magnitude Δ_0.

We note that Monien *et al.*[22] have recently reported results for thermodynamic properties of "d-wave" states, including the state (3.1), in agreement with ours with the exceptions detailed below.

For convenience, we have assumed a spherical Fermi surface for calculating angular averages, even for those states compatible with hexagonal symmetry. In principle, $\hat{\mathbf{k}}$ in (3.1) and (3.2) should be replaced with the Fermi velocity $v_{\mathbf{k}}$ and integrals performed over the true Fermi surface. However, we expect that results at low temperature will be insensitive to the details of the Fermi surface, given a particular gap structure. This statement may apply qualitatively even in the case of an order parameter with the exact (unbroken) symmetry of the underlying lattice and "quasinodes" created by a pair potential which varies by factors of 10–100 over the Fermi

surface, following a highly anisotropic effective mass. In this case, Δ_k would have to be renormalized, as in the usual Abrikosov-Gor'kov theory of impurity scattering.

B. Density of states

Anisotropic order parameters are conveniently characterized by the density of single-particle excitations, given in the case of particle-hole symmetry by

$$\frac{N(\omega)}{N_0} = -\,\mathrm{Im}G_0\ , \tag{3.3}$$

where G_0 is determined by solving Eq. (2.8a) self-consistently.

In Figs. 1(a) and 1(b), we plot $N(\omega)/N_0$ for polar and axial states in the presence of various impurity concentrations and scattering strengths. Above a critical energy $\omega_c \simeq \gamma^{1/2}\Delta_0$, where $\gamma \equiv \Gamma/\Delta_0$, self-consistency is unnecessary, and the curves display the ω and ω^2 behavior expected for the pure polar and axial states, respectively. Below this frequency in the unitary limit $c=0$, a peak is observed centered on zero frequency, the analog of the bound state in the gap found in calculations of resonant scattering in ordinary superconductors.[24–27] For small deviations from the unitarity limit, the peak position shifts to finite frequency and eventually disappears. For weak scattering ($c \gg 1$) the results become asymptotically those of Ueda and Rice[28] for impurity scattering in anisotropic superconductors in the Born approximation.

For an axial state, a small-energy expansion of (2.8a) shows that $N(0)$ is finite for concentrations and scattering strengths such that $\gamma > (2/\pi)c^2$, and hence is finite for infinitesimal impurity concentration in the unitarity limit. The same is true for the polar state even for weak scattering, as first demonstrated by Ueda and Rice[28] and Gor'kov.[29] The dependence of $N(0)$ on γ and c is given by

$$\frac{N(0)}{N_0} = \frac{y}{\tan y} \equiv f_1(y) \quad \text{(axial)}\ ,$$
$$\frac{N(0)}{N_0} = \frac{y}{\sinh y} \equiv f_2(y) \quad \text{(polar)}\ , \tag{3.4}$$

where y is the solution of $f_i^2(y) = \gamma y - c^2$. The limiting behavior of $N(\omega)$ for $\omega < \omega_c$, which determines, e.g., the specific heat of the system at the lowest temperatures, can vary dramatically with small deviations from the unitary limit. For example, in an axial-like state, $N(\omega) \sim N(0)$ for $\gamma \gg c^2$, $N(\omega) \sim \omega^{1/2}$ for $\gamma \sim c^2$, and $N(\omega) \sim \omega^2$ for $\gamma \ll c^2$, provided $\gamma \ll 1$. In a polarlike state, $N(\omega) \sim N(0) + ac^2\omega$ for all $\gamma \ll 1$, where $a = a(\gamma, c)$ is a constant.

In Figs. 1(c) and 1(d) we plot $N(\omega)/N_0$ for the hybrid and hexial states. In both the intermediate and "gapless" frequency ranges discussed above, the hybrid state is seen to yield results qualitatively very similar to the polar state, due to the presence of line nodes which dominate the low-energy behavior. Similarly, the hexial state mimics an axial-state behavior for frequencies $\omega < \omega_h$, where the scale ω_h is set by the ratio Δ_1/Δ_2, here taken to be 1.

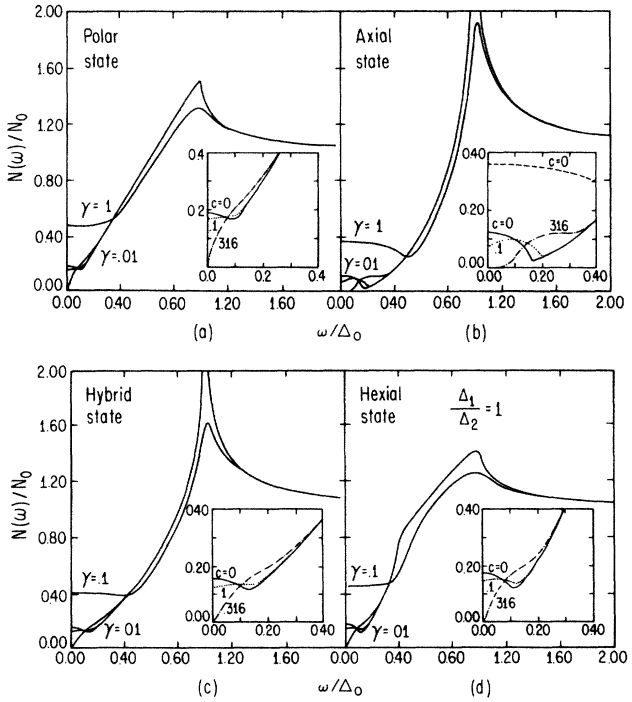

FIG. 1. Quasiparticle density of states $N(\omega)/N_0$ vs reduced energy ω/Δ_0. Solid lines in main figures are $c=0$, $\gamma \equiv \Gamma/\Delta_0 = 0.01$, 0.1. Insets show variation at low energy with cotangent of scattering phase shift $c=0$, 0.1, 0.316. (a) Polar state; (b) axial state; (c) hybrid state; (d) hexial state.

C. Critical temperature and order parameter

In order to calculate temperature-dependent quantities, we need to know the behavior of the critical temperature T_c and the gap magnitude $\Delta_0(T/T_c)$ as a function of γ and c. The former is determined as usual by solving the gap equation (2.10) for $\Delta_0 \to 0$. The T_c suppression found is the usual Abrikosov-Gor'kov result,[30]

$$\ln\left[\frac{T_c}{T_{c0}}\right] = \psi(\tfrac{1}{2}) - \psi\left[\frac{1}{2} + \frac{\Gamma_N}{2\pi T_c}\right]\ , \tag{3.5}$$

where $\Gamma_N \equiv \Gamma/(1+c^2)$ is the scattering rate in the normal state and ψ is the digamma function. In the unitary limit the pair-breaking parameter $\alpha_c \equiv \Gamma_N/2\pi T_c$ is roughly given by $n_i T_F/T_c$. Assuming $T_F \cong 10^4(m/m^*)T_c$, a concentration of a few percent should destroy superconductivity altogether, as is actually observed in UPt_3.[31] On the other hand, T_c will be only slightly depressed if impurity concentrations remain at the 10^{-3}–10^{-4} level considered characteristic of nominally pure samples.[32] Thus (Γ/T_c)'s of the order of 0.01–0.1 should be relevant to our analysis of the existing experimental results on "pure" heavy-fermion superconductors.

At the small concentrations we consider here, the gap parameter Δ_0 is also depressed only slightly. In Fig. 2, we show the results of a numerical solution of (2.10) for a polar state for various values of Γ and c. Results for axial and other states are similar. It is easy to show analytically that, for all states, Δ_0 is depressed linearly in order Γ/T_c for small n_i. In addition, expansion of (2.10) near T_c yields results for the weak-coupling specific-heat

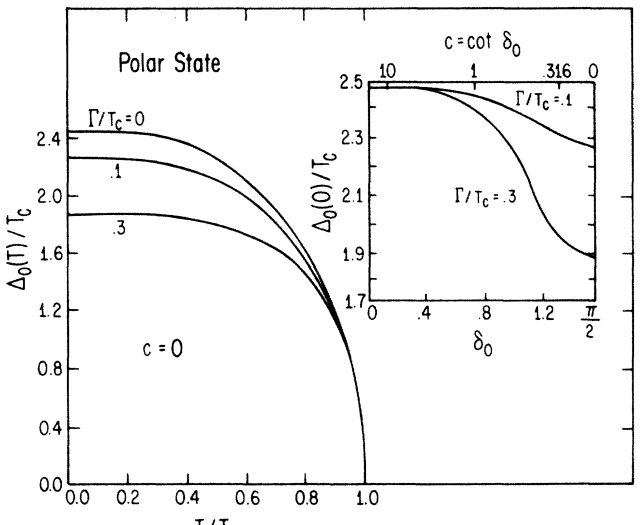

FIG. 2. Order-parameter magnitude Δ_0/T_c vs temperature T/T_c for a polar state, $\Gamma/T_c=0$, 0.1, 0.3 at $c=0$, $\Delta_0(0)/T_c$ vs phase shift δ_0, $\Gamma/T_c=0.1$, 0.3.

jumps for axial and polar order parameters,

$$\frac{\Delta C}{C_N}=\frac{12[1-\alpha_c\psi^{(1)}(\alpha_c+\frac{1}{2})]}{\left[\frac{\mu}{6}\alpha_c\psi^{(3)}(\alpha_c+\frac{1}{2})-b\psi^{(2)}(\alpha_c+\frac{1}{2})\right]}, \tag{3.6}$$

where $\mu\equiv(1-c^2)/(1+c^2)$ and $b=\frac{3}{5}$ for an axial state, $\frac{9}{10}$ for a polar state, and $\frac{5}{7}$ for a hybrid state. Here $\psi^{(n)}(x)$ is the nth derivative of the Γ function. To illustrate the effects of unitary scattering, we plot in Fig. 3 $\Delta C/C_N$ for two values of the scattering rate, $\Gamma/T_c=0.1$ and 0.5, for polar and axial states.

D. Specific heat

The specific heat of a weak-coupling superconductor is most conveniently calculated from the entropy. In a pure superconductor, the thermodynamically important excitations are the Bogoliubov quasiparticles, which are eigenstates of momentum $\mathbf{k}$ and spin σ (in the absence of spin-orbit interactions). For the purpose of calculating the entropy, these excitations may be considered to be independent (the residual interaction of the Bogoliubov quasiparticles, which among other things gives rise to their finite lifetime, leads to negligible corrections to the limiting low-temperature entropy). The entropy is then given by the usual combinational expression for a Fermi gas of particles with energy $E_{\mathbf{k}}$.

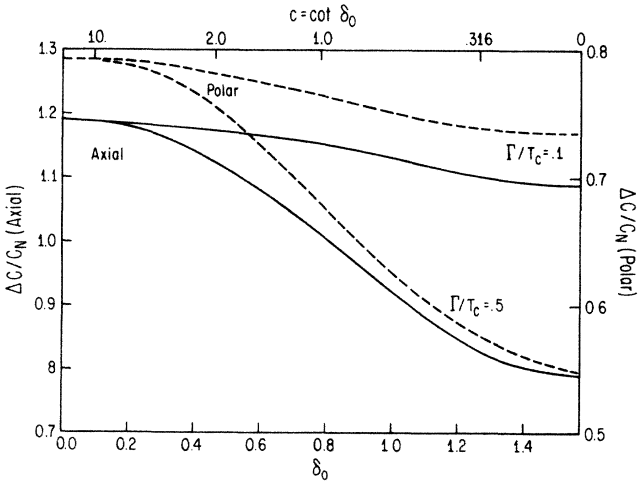

FIG. 3. Normalized specific-heat jump $\Delta C/C_N$ for axial and polar states vs phase shift δ_0, for $\Gamma/T_c=0.1$ and 0.5.

In the presence of impurity scattering, momentum is no longer a good quantum number. Rather, the Bogoliubov quasiparticles are now energy eigenstates in the presence of an impurity potential with eigenvalues E_n. These eigenstates are obtained as solutions to the Bogoliubov–de Gennes equations.[33] The important thing to notice is, however, that inasmuch as the impurity scattering is elastic, the Bogoliubov quasiparticles can still be considered independent excitations, for the same reasons as in the pure case. This is true as long as the presence of impurities does not affect the validity of mean-field theory which does not occur until much higher concentrations than we consider here. Their entropy is therefore still that of a system of independent fermions, with energy E_n in states labeled by n, and is hence given by

$$S=-2k_B\sum_n[f_n\ln f_n-(1-f_n)\ln(1-f_n)]\,. \tag{3.7}$$

Here $f_n=f(E_n)$ is the Fermi function, and the factor 2 in (3.7) accounts for the spin degrees of freedom. Introducing the density of states $N(\omega)$, defined by

$$N(\omega)=2\sum_n\delta(\omega-E_n)\,, \tag{3.8}$$

one can rewrite (3.5) as

$$S=-k_B\int_0^\infty d\omega\,N(\omega)[f\ln f-(1-f)\ln(1-f)]\,, \tag{3.9}$$

where now $f=f(\omega)$. Note that $N(\omega)$ is a T-dependent quantity here.

The specific heat follows from (3.9) by differentiation with respect to temperature as

$$C=T\frac{dS}{dT}=2\int_0^\infty d\omega\left[\frac{N(\omega)\beta^2\omega^2e^{\beta\omega}}{(e^{\beta\omega}+1)^2}-\beta\frac{dN(\omega)}{d\beta}\left[\ln(1+e^{-\beta\omega})+\frac{\beta\omega}{e^{\beta\omega}+1}\right]\right] \tag{3.10}$$

where $\beta=1/k_BT$. This is a rather involved expression, due to the temperature dependence of the density of states.

In Fig. 4, we plot the specific heat versus temperature for various states. Figures 4(a) and 4(b) show the variation of C/T for polar and axial states with scattering phase shift and concentration. As remarked in I, the crucial feature is an offset in the $T\to0$ limiting value of

C/T, reflecting the finite zero-energy density of states, even for surprisingly low impurity concentrations. In Ref. 34 data on UPt_3 (see also Refs. 35 and 36) were fitted to the laws $C(T)=\alpha T+\beta T^2$ below $\sim 0.3T_c$. If one then extrapolates linearly to 0 while maintaining entropy balance, C/T is finite at $T=0$, corresponding to $\gamma \sim 0.03$ for a polar state in the unitary limit. In Fig. 4(c), we plot C/T for all four states considered here. We note that, although C/T in all cases does essentially reflect the corresponding density of states, distinguishing between states with points and lines of nodes in the order parameter on the basis of one-particle properties may prove extremely difficult, except in very pure samples.

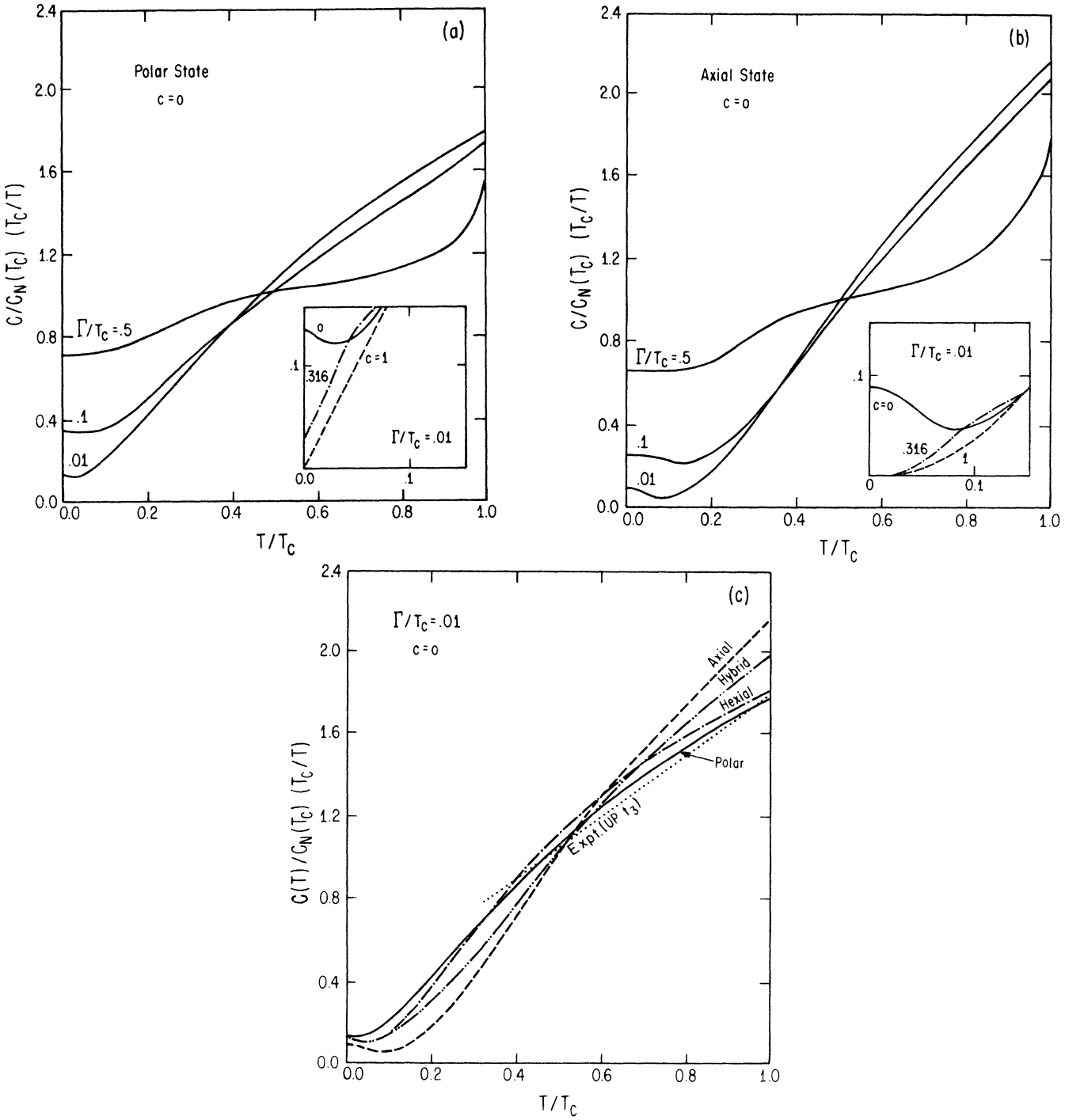

FIG. 4. Normalized specific heat CT_c/C_NT for axial and polar states vs reduced temperature T/T_c. (a) and (b) For $c=0$, $\Gamma/T_c=0.01$, 0.1, 0.5. Inset shows variation with cotangent of scattering phase shift $c=0$, 0.316, 1 for $\Gamma/T_c=0.01$. (c) CT_c/C_NT for $\Gamma/T_c=0.01$, $c=0$ for axial (dashed line), hexial (dashed-dotted), hybrid (dashed–double-dotted), and polar (solid) states. Dotted line: data of Ref. 34 on UPt_3.

We have derived the specific heat from a weak-coupling theory, assuming a spherical Fermi surface. The jumps $\Delta C/C$ shown in Fig. 4 are therefore determined by the weak-coupling coefficients in the Ginzburg-Landau (GL) expansion of the BCS free energy near T_c. Were the heavy-fermion systems in question really weakly-coupled and anisotropic, only that single state with the highest T_c (corresponding to a given representation) would be thermodynamically stable; other states are, in this case, energetically unfavorable. Here we adopt the point of view that, while strong-coupling corrections to the GL coefficients are likely to be small in UPt_3, there is no reason to suppose that band-structure anisotropy corrections will be negligible. Thus a polarlike state may well be stabilized with respect to an axial state by Fermi-surface anisotropy, just as in ^{3}He the ABM (axial) state is stabilized with respect to the BW (isotropic) state by strong-coupling corrections. The quantitative values of the specific-heat jumps plotted—as opposed to the qualitative low-temperature behavior—should therefore not be taken as the basis of a realistic comparison with experiment. In particular, the apparent near agreement of the theoretical $\Delta C/C_N$ for the polar state and the experimental jump for UPt_3 must be regarded as accidental.

E. Thermal conductivity

The thermal conductivity κ of an anisotropic superfluid state is in general a tensor quantity. It can be expressed in terms of the heat-current response function by a Kubo formula. Generalizing the treatment given for an s-wave superconductor[37] we find the heat conductivity tensor as

$$\kappa_{ij}=\kappa_N(T)\left[\frac{9}{4\pi}\right]\int_0^\infty \frac{d\omega}{T}\left[\frac{\omega}{T}\right]^2 \times \operatorname{sech}^2\left[\frac{\omega}{2T}\right]\mathrm{Re}[\chi^{ij}_{\underline{Q}\underline{Q}}(\omega)]\ . \tag{3.11}$$

Here $\kappa_N(T)=\frac{1}{3}C_N v_F^2\tau$ is the heat conductivity in the normal state and

$$\chi^{ij}_{\underline{Q}\underline{Q}}(\omega)=\frac{\Gamma}{\pi}\int\frac{d\Omega}{4\pi}\int d\xi_k\,\overline{\mathrm{Tr}[\underline{Q}^i\underline{g}(\omega+i0)\underline{Q}^j\underline{g}(\omega-i0)]}\ , \tag{3.12}$$

where the overbar denotes an impurity average and $\underline{Q}^i=\hat{\mathbf{k}}_i\underline{\tau}^3$ is the bare vertex. The trace is over Nambu matrices. The response function χ_{QQ} has been defined to be dimensionless, with limiting value $\chi_{QQ}\to\frac{2}{3}$ in the limit of large frequencies and/or in the normal state. The definition of χ_{QQ} in (3.12) coincides with the general definition of the response function χ_{AB} in Appendix B. Using the definitions introduced there and the results for vertices of odd symmetry under $\mathbf{k}\to-\mathbf{k}$, we have

$$\chi^{ij}_{\underline{Q}\underline{Q}}(\omega)=\langle\hat{\mathbf{k}}_i\hat{\mathbf{k}}_j L^{33}\rangle_{\hat{\mathbf{k}}}+\sum_{n=1,2}\langle\hat{\mathbf{k}}_i L^{3n}\rangle_{\hat{\mathbf{k}}}\Lambda_{nm}\langle\hat{\mathbf{k}}_j L^{m3}\rangle_{\hat{\mathbf{k}}}\ , \tag{3.13}$$

with L^{ij} given by (B2), and (B5), and (B7), and Λ_{nm} defined in (B13). Note that the vertex corrections, i.e., the last term in (3.13), vanish for even-parity pairing, due to the even parity of the Green's functions and the quantities L^{ij}. For odd-parity pairing, there is in general a contribution from the vertex corrections to κ. It is worth noting that for uniaxial states the largest eigenvalue is unrenormalized. This is because the quantity $\langle\hat{\mathbf{k}}L^{3n}\rangle_{\hat{\mathbf{k}}}$, $n=1,2$, vanishes for certain symmetry directions; these are, e.g., $\hat{\mathbf{q}}\perp\hat{\boldsymbol{l}}$ for the polar state and $\hat{\mathbf{q}}\|\hat{\boldsymbol{l}}$ for the axial state, where $\hat{\mathbf{q}}$ is the direction of the thermal gradient. In each case, the smallest eigenvalue, $\kappa_{\min}$, is renormalized, but the effect is relatively large only at the smallest energies at the impurity concentrations considered here; in this energy range the conductivity $\kappa_{\min}$ is in any case too small to be experimentally observable. Thus for the small impurity concentrations we discuss, the effect of vertex corrections is negligible, except perhaps on the anisotropy $\kappa(\hat{\mathbf{q}};T)$ at the lowest temperatures. Here vertex corrections will be of relative order $(\hat{\mathbf{q}}\cdot\hat{\mathbf{n}})^2$, where $\hat{\mathbf{n}}$ is the direction of gap nodes, with respect to the bare bubble. Similarly, the effect of renormalized single-particle energies $\tilde{\xi}$ not considered in I is negligible, except for changes of $\sim 10\%$ for values $c\sim 1$. In this case the off-diagonal elements k_{ij}, $i\neq j$, also become appreciable, as mentioned above.

In Fig. 5 we plot the eigenvalues κ_{xx} and κ_{zz} calculated from (3.11) and (3.13) for the states considered here, and compare with experimental data on UPt_3.[34,38] In no case do we find substantially better agreement than in I comparing the naive average $\bar{\kappa}=\mathrm{Tr}\vec{\kappa}=\frac{2}{3}\kappa_{xx}+\frac{1}{3}\kappa_{zz}$ with experiment, although the hexial results are somewhat closer to the experimental results on polycrystalline samples at low T. It seems clear, however, that while this average is appropriate at high temperatures, where all eigenvalues of $\vec{\kappa}$ are of similar magnitudes, it is suspect at low temperatures where $\vec{\kappa}$ is highly anisotropic. In this case, a model of the polycrystalline superconductor consisting of grains of fixed, randomly oriented $\hat{\boldsymbol{l}}$ directions leads to the conclusion that grains with $\hat{\boldsymbol{l}}$ optimally oriented to conduct heat flow will dominate the conductivity. Thus we expect a crossover from $\bar{\kappa}$ at high temperatures to $\kappa_{\max}$ at lower T in polycrystalline samples; this improves the qualitative fit to experiment of the resonant scattering model, although deciding among the various candidate states remains problematic. Note that the existing data on UBe_{13} follow a T^2 law from T_c down to the lowest temperatures.[39,40]

F. Nuclear magnetic relaxation rate

The calculation of the nuclear magnetic relaxation rate T_1^{-1} in an impure superconductor has been reviewed by Maki.[41] Assuming a contact nuclear matrix element, T_1^{-1} is proportional to the imaginary part of the electronic spin-spin correlation function evaluated at the nucleus,[42]

$$(T_1T)^{-1}\propto\frac{1}{\Omega_0}\mathrm{Im}\langle[\mathbf{S}(\mathbf{r}),S(\mathbf{r},\Omega_0)]\rangle = \frac{1}{\Omega_0}\mathrm{Im}\left[T\sum_{\omega_n}\sum_{\mathbf{k}\mathbf{k}'}\mathrm{Tr}[\underline{\alpha}^i\underline{g}(\mathbf{k}\omega_n)\underline{\alpha}^i\underline{g}(\mathbf{k}'\omega_n+i\Omega_0)]\right]\ , \tag{3.14}$$

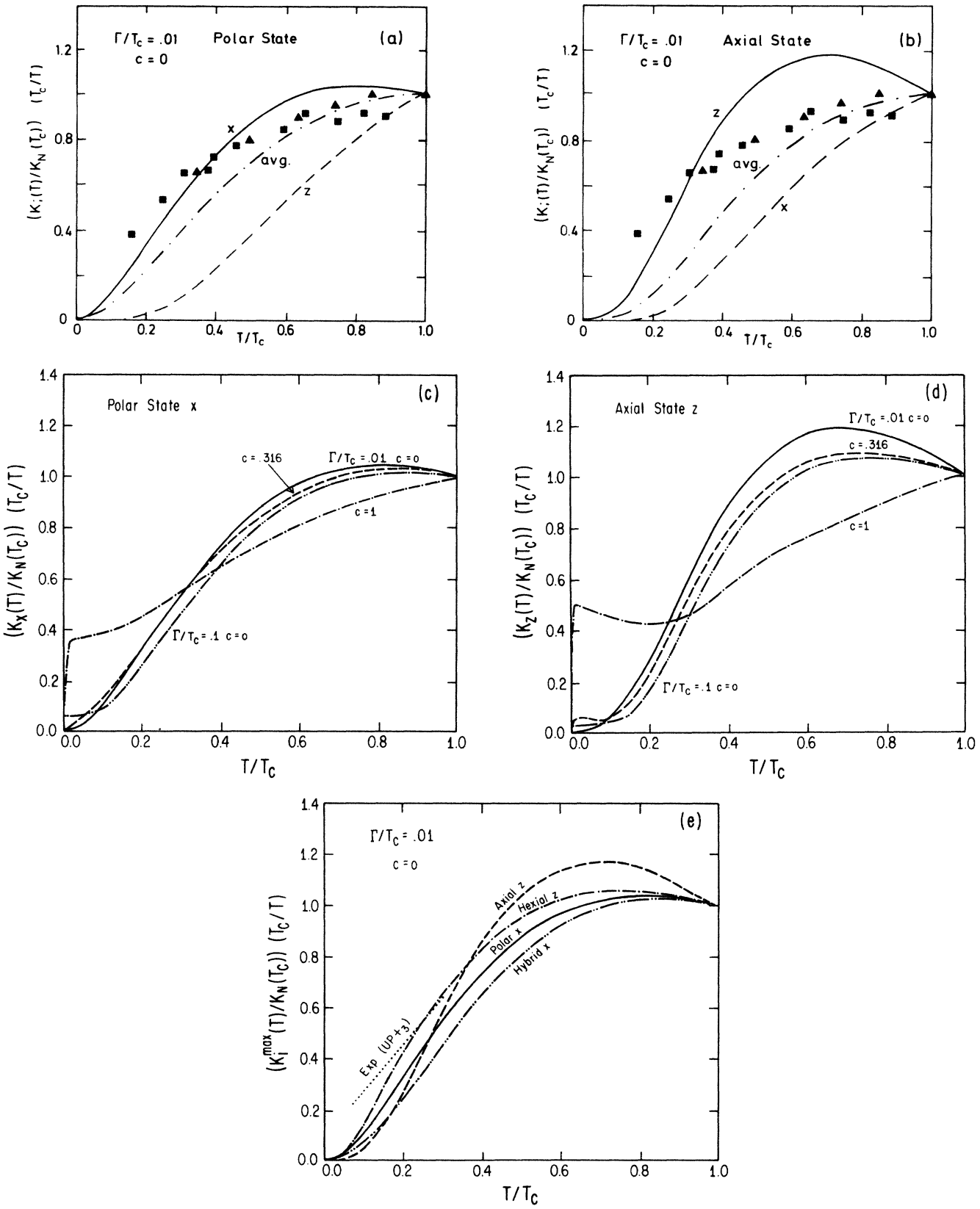

FIG. 5. Normalized thermal conductivity $K_i(T)T_c/K_NT$ vs T/T_c. (a) and (b) For polar and axial states, $\Gamma/T_c=0.01$, $c=0$. Solid lines represent κ_{max}, dashed κ_{min}, and dashed-dotted the naive average conductivity $\bar{\kappa}=\frac{2}{3}\kappa_{xx}+\frac{1}{2}\kappa_{zz}$. Triangles and squares are data of Refs. 34 and 38 on UPt_3. (c) and (d) Variation of $\kappa(T)/T$ vs T with cotangent of scattering phase shift $c=0$, 0.316, 1 with $\Gamma/T_c=0.01$, 0.1. κ_{max} is the largest eigenvalue of $\bar{\kappa}$ for polar and axial states, respectively. (e) Maximum eigenvalue κ_{max} as indicated vs T for axial, polar, hexial, and hybrid states, $\Gamma/T_c=0.01$, $c=0$. Dotted line is low-T fit from Ref. 34.

where Ω_0 is the Larmor frequency and $\underline{\alpha}^i \equiv \mathrm{diag}(\sigma_i, -\sigma_i^T)$ is the electronic spin operator in particle-hole space. Since by assumption $G_{12}=0$, only the τ^0 components of $\underline{g}$ contribute to the momentum sums:

$$(T_1T)^{-1} \propto (2\pi N_0)^2 \frac{1}{\Omega_0} \mathrm{Im} \left[T \sum_{\omega_n} G_0(\omega_n) G_0(\omega_n + i\Omega_0) \right] . \tag{3.15}$$

This expression may be most easily evaluated by using a spectral representation for G_0,

$$G_0(\omega) = \frac{1}{N_0} \int d\omega' \frac{N(\omega')}{\omega - \omega' - i0} . \tag{3.16}$$

Performing the analytical continuation and taking the limit $\Omega_0 \to 0$ yields finally

$$\frac{T_1^{-1}}{(T_1^{-1})_N} = 2\frac{T}{T_c} \int_0^\infty d\omega \left[\frac{-\partial f}{\partial \omega} \right] \left[\frac{N(\omega)}{N_0} \right]^2 , \tag{3.17}$$

where $(T_1^{-1})_N$ is the normal-state relaxation rate at T_c. Unlike the other two-particle properties discussed here, the bare spin-spin correlation function in (3.14) does not have to be supplemented by the addition of vertex corrections.[43]

In Fig. 6 we have plotted $(T_1T)^{-1}$ for axial and polar states in the unitary limit. Unfortunately, at this writing an NMR signal has been observed only in UBe_{13}, for which none of the states discussed here is appropriate. Furthermore, direct comparison with experiment is problematic in this case, as remarked in the Introduction. Nevertheless, one striking aspect of the experiment of McLaughlin *et al.*[4] seems worthy of comment. Below $\sim 0.2T_c$, the observed power-low temperature dependence of T_1^{-1} is observed to cross over to a roughly linear behavior characteristic of the normal-state Korringa relaxation. This is exactly what one expects in the presence of resonant scatterers, as seen from the figure. Thus resonant scattering in an anisotropic superconducting state provides an alternative explanation to the new low-energy relaxation mechanism invoked by the authors to explain their data.

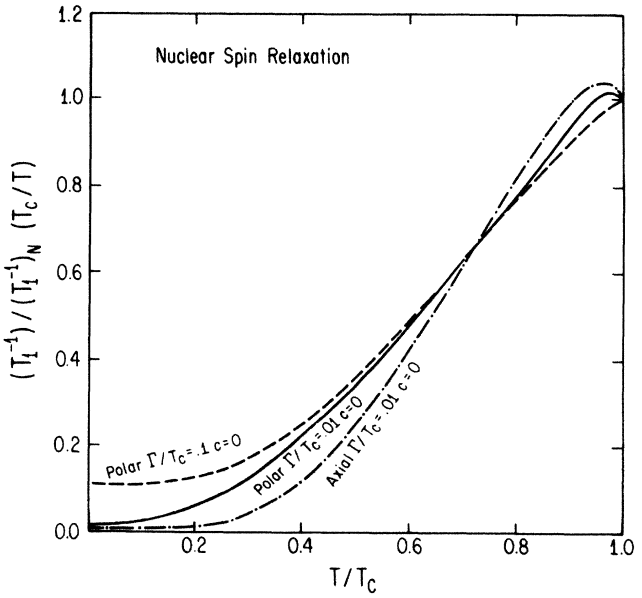

FIG. 6. Nuclear-spin relaxation rate $T_cT_1^{-1}/TT_{1N}^{-1}$ vs temperature T/T_c for polar and axial states in the unitary limit, $c=0$, $\Gamma/T_c=0.01$, 0.1.

IV. CONCLUSIONS

There are a number of pieces of evidence indicating that resonant scattering impurities are present in all heavy-fermion superconductor samples grown to date, and play an important role in the thermodynamic and transport properties of the anisotropic states we consider here. Perhaps the most compelling argument is that, as of this writing, no other explanation for the strong (but non-BCS) temperature dependence of transport properties, and particularly the thermal conductivity, has been put forward. Given the highly anisotropic nature of the superconducting state, a hypothesis qualitatively consistent with all experiments on heavy-fermion systems thus far performed, impurity-limited transport properties deviate strongly from their normal-state behavior at low temperatures only in the presence of strong (near-unitary scatterers).

In addition, "offsets," or finite low-temperature limiting values of κ/T and C/T in UPt_3, strongly suggest a finite density of zero-energy quasiparticle excitations. This is possible in ordinary gapless superconductors, but only at impurity concentrations so large as to nearly destroy superconductivity. While we have been reluctant to apply the theory described herein directly to UBe_{13} because of the strong energy dependence of normal-state quantities, a similar offset in $(T_1T)^{-1}$ is highly suggestive. Ott *et al.*,[44] while claiming no offset in a fit to UBe_{13} specific-heat data, find that near-resonant scattering in a state with point nodes does provide a good fit to experiment.

Our investigation of various more realistic states consistent with the hexagonal symmetry of the UPt_3 crystal has not substantially improved quantitative agreement with experiment. This is perhaps not surprising, considering our neglect of Fermi-surface anisotropy, known to be large in UPt_3.[45] This enters not only in the usual Fermi-surface integrals, but through arbitrary functions with D_6 symmetry, here taken to be unity, with which each of the states, e.g., (3.1) and (3.2), may be multiplied.

What is clearly needed is a systematic measurement of specific-heat and transport properties at larger impurity concentrations, preferably in single crystals to avoid averaging ambiguities like those discussed in Sec. III E. Observation of increasing values of κ/T as $T \to 0$ for increasing impurity concentrations would provide strong support for the hypotheses advanced here. On the other hand, if low-temperature transport and specific heat were observed to decrease with increasing doping levels, this would almost certainly imply filling in of gap nodes, contradicting the assumption of symmetry-enforced nodal structure ($G_{12}=0$) made here. Impurity scattering

in this case might well still be unitary, but a somewhat more complicated treatment involving self-consistent order-parameter renormalization would be necessary.

It has proven difficult to identify the nodal structure of the heavy-fermion gap from temperature dependencies of thermal properties alone. A more important tool in this regard may be hydrodynamic sound-attenuation measurements, a discussion of which we reserve for a later work.[21] Here one has two external directions, ultrasound polarization and wave vector, with which gap anisotropy may be probed. The calculation is complicated, however, by the important role played by vertex corrections, due to both pair and impurity scattering. The former must be included to maintain gauge invariance, because in the anisotropic state the stress-tensor correlation function determining the attenuation couples to the density. In addition, novel relaxation mechanisms may contribute to attenuation over the entire temperature range.[46]

Finally we mention that we have, until now, no microscopic basis for the assumption of resonant scattering in these systems. An understanding of this phenomenon may prove essential to the understanding of heavy-fermion superconductivity itself.

ACKNOWLEDGMENTS

One of the authors (P.H.) would like to thank the Walther-Meissner-Institut of the Bavarian Academy of Sciences, Munich, and the Department of Physics at the University of Florida for financial support. Partial support by Deutsche Forschungsgemeinschaft during the early stages of this work is also gratefully acknowledged. The work of P.W. was partially supported by the National Science Foundation under Grant No. DMR-8607941. Numerical work was performed on the University of Florida NERDC system and the UC–San Diego supercomputer.

APPENDIX A: SELF-CONSISTENT TREATMENT OF *s*-WAVE SCATTERING

In this appendix we show that the $\underline{\tau}_3$ component of the integrated Green's functions $\underline{G}$ defined after Eq. (2.6) may be neglected in a self-consistent treatment of any system with particle-hole symmetry in the presence of *s*-wave scatterers. Relaxation of the particle-hole symmetry requirement, or inclusion of higher-order angular-momentum waves in the scattering matrix element, makes the solution of the Dyson equation (2.1) considerably more difficult. We note as well that the argument for the consistency of the assumption $G_1=G_2=0$ in the case of order parameters odd under certain crystal symmetry transformations exactly follows that given here for G_3.

The formal solution to (2.1) given in (2.7) shows that impurities shift the poles in the single-particle Green's function to renormalized quasiparticle energies $\tilde{\omega}^2=\tilde{\xi}_{\mathbf{k}}^2+\tilde{\Delta}_{\mathbf{k}}^2$, where $\tilde{\omega}$, $\tilde{\xi}_{\mathbf{k}}$, and $\tilde{\Delta}_{\mathbf{k}}$ are as defined in (2.8). In the Born approximation for the self-energy Σ due to spinless *s*-wave scatterers, one has

$$\underline{\Sigma}(\mathbf{k},\omega)=\sum_{\mathbf{k}'} V(\mathbf{k},\mathbf{k}')G(\mathbf{k}',\omega)V(\mathbf{k}',\mathbf{k})$$
$$=|V|^2\int\frac{d\Omega'}{4\pi}\int d\xi\, N(\xi)\left[\frac{\tilde{\omega}\underline{\tau}^0+\tilde{\xi}^2\underline{\tau}^3+\tilde{\underline{\Delta}}_{\mathbf{k}'}}{\tilde{\omega}^2-\tilde{\xi}^2-\tilde{\Delta}_{\mathbf{k}'}^2}\right], \tag{A1}$$

where the second equality follows from the assumed momentum independence of the scattering potential V. In the particle-hole–symmetric case, we may replace the energy-dependent density of states $N(\xi)$ to a very good approximation by N_0, and note that

$$\Sigma_3=|V|^2N_0\int d\xi\frac{\tilde{\xi}}{\tilde{\omega}^2-\tilde{\Delta}^2-\tilde{\xi}^2}=0 \tag{A2}$$

is a self-consistent solution to (A1). In the T-matrix approximation, however, $\Sigma_3=0$ is no longer a consistent solution since $\underline{\Sigma}$ is no longer proportional to $\underline{G}$, even in the case of *s*-wave scattering [cf. Eq. (2.12)]. In fact, inspection of (2.6) shows that $\Sigma_3\propto T_3=0$ is not a consistent solution under any circumstances.

Nonetheless we show here that, under the assumption of particle-hole symmetry, $\tilde{\xi}_{\mathbf{k}}$ may be replaced by the bare single-particle spectrum $\xi_{\mathbf{k}}$ in all expressions for single-particle properties, and that G_3 may always be taken to vanish. The corresponding component of the self-energy, Σ_3, is nonzero but plays no role in the calculation of single-particle quantities.

We begin by considering the quantity

$$G_3(\omega)\equiv\frac{1}{\pi N_0}\sum_{\mathbf{k}} g_3(\mathbf{k},\omega)$$
$$=\frac{1}{\pi}\left\langle\int_{-\infty}^{\infty}d\xi\frac{\xi+\Sigma_3}{(\omega-\Sigma_0)^2-(\xi+\Sigma_3)^2-\Delta_{\mathbf{k}}^2}\right\rangle_{\hat{\mathbf{k}}}, \tag{A3}$$

where we have explicitly exhibited the definitions (2.8) of $\tilde{\xi}$ and $\tilde{\omega}$, but taken $\Delta_{\mathbf{k}}$ to be unrenormalized for simplicity. The consistency of the last assumption follows from arguments identical to the present one, as mentioned above. Note that particle-hole symmetry has been assumed in the second equality in (A3). Continuing the integration into the complex ξ plane, we see that the integrand has poles at $\pm\xi_0-\Sigma_3$, where $\xi_0\equiv\pm[(\omega-\Sigma_0)^2-\Delta_k^2]^{1/2}$, as shown in Fig. 7(a). We may transform the variable of integration to $\tilde{\xi}\equiv\xi+\Sigma_3$ at the cost of transforming the contour of integration C in Fig. 7(a) away from the real axis. If Σ_3 is such that the transformed contour lies between the two poles, as does, for example, the contour $\tilde{C}_1$ in Fig. 7(b), the contour may be rotated to $\tilde{C}_1'$ so as to pass through the origin. In this case $G_3=0$ because the integrand in (A3) is odd in $\tilde{\xi}$. It remains only to show that the situation represented by contour $\tilde{C}_2$ [Fig. 7(b)], where the contour passes outside of both poles $\tilde{\xi}=\pm\xi_0$, never occurs. The proof is a self-consistent one. If $G_3=0$, the T-matrix may be shown to have the simple form (2.12). The self energy $\underline{\Sigma}$ is then proportional to $\underline{T}$ through Eq. (2.2):

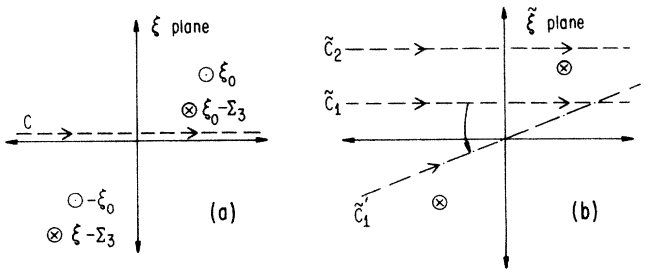

FIG. 7. Poles and integration contours of G_3 in the complex ξ plane.

$$\Sigma_0'' = \mathrm{Im}\left[\frac{\Gamma G_0}{c^2 - G_0^2}\right] = \Gamma\left[\frac{G_0''}{(c-G_0')^2+(G_0'')^2} + \frac{G_0''}{(c+G_0')^2+(G_0'')^2}\right], \tag{A4a}$$

$$\Sigma_3'' = \mathrm{Im}\left[\frac{-\Gamma c}{c^2 - G_0^2}\right] = -\Gamma\left[\frac{G_0''}{(c-G_0')^2+(G_0'')^2} - \frac{G_0''}{(c+G_0')^2+(G_0'')^2}\right]. \tag{A4b}$$

Thus

$$|\Sigma_3''| < |\Sigma_0''| \ . \tag{A5}$$

Furthermore, it is a matter of straightforward algebra to show that $|\xi_0''| > |\Sigma_0''|$. Therefore

$$|\xi_0''| > |\Sigma_3''| \ , \tag{A6}$$

from which it follows that contours of the type $\tilde{C}_2$ never occur. As argued above, G_3 must therefore vanish, consistent with the original assumption. It is somewhat more tedious but straightforward to show that $G_3 \neq 0$ is *not* a consistent solution of (A3).

APPENDIX B: VERTEX CORRECTIONS TO TWO-PARTICLE CORRELATION FUNCTIONS

In this appendix we calculate the vertex corrections to two-particle properties in the superconducting state. These are seldom discussed in the literature on ordinary superconductivity, since they vanish identically for an isotropic gap parameter Δ in the simplest s-wave scattering approximation. In an anisotropic superconductor this need not be the case, as pointed out recently by Scharnberg *et al.*[12] Nevertheless, we show here that vertex corrections may still be neglected in a large number of cases when the response function and order parameter obey certain symmetries. The most important exceptions are the longitudinal components of the stress-tensor–stress-tensor correlation function needed to calculate the deformation-potential contribution to longitudinal sound attenuation in the hydrodynamic limit. Here vertex corrections are always important. The expressions given by Scharnberg *et al.*[12] are, however, inconsistent with the Dyson equation (2.1) due to a failure to properly renormalize the single-particle energy spectrum, as discussed in Sec. II (see, however, Ref. 23). Because of unphysical divergences in certain components of the vertex function which result if Σ_3 is arbitrarily taken to be zero, large errors in the calculated attenuation may occur even very close to the unitarity limit $c=0$. We discuss this point in more detail in Ref. 21. Here we give a general solution for the two-particle vertex function for s-wave scattering.

To calculate vertex corrections to two-particle correlation functions due to independent scatterings of electrons and holes from impurities, we use the formalism developed by Baym.[47] The retarded correlation function between operators $\underline{A}(\hat{\mathbf{k}};\mathbf{q},\Omega)$ and $\underline{B}(\hat{\mathbf{k}};\mathbf{q},\Omega)$ is depicted in Fig. 8. All solid lines represent full Green's functions, and Greek letters are taken to label the particle-hole indices. The full vertex part Λ is then related to the particle-hole irreducible vertex $\underline{I} \equiv \delta\Sigma/\delta G$ through the integral equation shown in Fig. 9. The irreducible vertex is fully determined when one has chosen a particular approximation for the self-energy, as shown in Fig. 10 for the T-matrix approximation used in the text.

Before solving the Bethe-Salpeter equation shown in Fig. 9 for Λ, it is useful to anticipate some properties of its solution. Since we always make the assumption that impurities are strongly screened, impurity interaction lines carry no momentum; consequently, none is transferred between particle and hole lines in the second diagram of Fig. 8. Thus the only internal momentum sums are over the momentum dependencies of the operators $\underline{A}$ and $\underline{B}$ and free propagators. In fact, the general expression for the correlation function $\langle[\underline{A},\underline{B}]\rangle$ is

$$\langle[\underline{A},\underline{B}]\rangle(q,\Omega=0) \equiv -\int \frac{d\omega}{T}\frac{\partial f(\omega)}{\partial\omega}\chi_{AB}(\omega) \ , \tag{B1}$$

where

$$\chi_{AB}(\omega) = \chi^0_{AB} + \frac{\Gamma^2}{(\pi N_0)^2}\left[\sum_{\mathbf{k}} A_{\beta\alpha}(\hat{\mathbf{k}}\cdot\hat{\mathbf{q}}) g_{\alpha\alpha_1}(\mathbf{k}_+\omega_+) g_{\beta_1\beta}(\mathbf{k}_-\omega_-)\right] \times \Lambda_{\alpha_1\beta_1;\alpha_2\beta_2}\left[\sum_{\mathbf{k}} g_{\alpha_2\alpha'}(\mathbf{k}_+\omega_+) g_{\beta'\beta_2}(\mathbf{k}_-\omega_-) B_{\alpha'\beta'}(\hat{\mathbf{k}}\cdot\hat{\mathbf{q}})\right], \tag{B1a}$$

where χ^0 is the response function with self-energy corrections only, all quantities are labeled by particle-hole indices as in Fig. 8, $\mathbf{k}_\pm \equiv \mathbf{k} \pm \frac{1}{2}\mathbf{q}$, $\omega_\pm \equiv \omega \pm i0^+$, and a sum over repeated indices is implied.

In ordinary (isotropic) superconductors, g is independent of direction on the Fermi surface. If $\underline{A}(\hat{\mathbf{k}}\cdot\hat{\mathbf{q}})$ or $\underline{B}(\hat{\mathbf{k}}\cdot\hat{\mathbf{q}})$ is then proportional to $P_l(\hat{\mathbf{k}}\cdot\hat{\mathbf{q}})$, $l \neq 0$, as is the case for many observables, corrections to χ^0_{AB} vanish

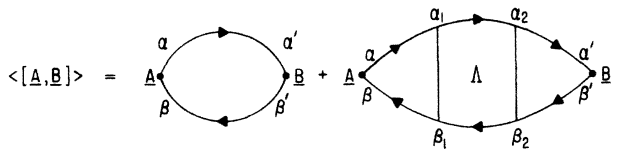

FIG. 8. Diagrams of the response function χ_{AB}.

identically as a result of the integration over angles. In an anisotropic system, however, the function

$$L_{\alpha\beta,\alpha'\beta'}(\hat{\mathbf{k}},\mathbf{q},\omega,\Omega)=\frac{\Gamma}{\pi}\int d\xi\, g_{\alpha\alpha'}\left[\mathbf{k}+\tfrac{1}{2}\mathbf{q},\,\omega+\frac{\Omega}{2}+i0\right]\times g_{\beta'\beta}\left[\mathbf{k}-\tfrac{1}{2}\mathbf{q},\,\omega-\frac{\Omega}{2}-i0\right] \tag{B2}$$

is angle dependent and may have an overlap with $A(\hat{\mathbf{k}}\cdot\hat{\mathbf{q}})$. However, some general cases may be identified in which $\langle \underline{A}L \rangle$ vanishes identically. For example, if A,B are given by a Legendre polynomial of odd order, all vertex corrections vanish in this approximation at $q=0$ for *even-parity* states. For example, both the Meissner kernel and the thermal conductivity are related to current-current correlation functions and are thus unrenormalized, provided $\Delta_k=\Delta_{-k}$. Even for odd-parity states, vertex corrections vanish for certain special symmetry directions of the wave vector $\hat{\mathbf{q}}$ relative to internal symmetry directions (gap axis). A similar statement may be made for the collision contribution to the transverse sound attenuation if the polarization and propagation vectors $\hat{\mathbf{e}}$ and $\hat{\mathbf{q}}$ are orthogonal and the symmetry axis of the order parameter lies along a direction of crystal symmetry. This follows since, in this case, the transverse component of the stress tensor is odd under reflection in some plane.

As an example, we sketch the derivation of the vertex corrections to the thermal conductivity (3.11). We are interested in the heat-current–heat-current response, with vertex $\underline{A}=\hat{\mathbf{k}}_i\tau^3$ (a factor ω has been split off). From (B1a) and (B2) we then have

$$\chi_{Q_iQ_j}=\chi^0_{Q_iQ_i}\delta_{ij}+\langle\hat{\mathbf{k}}_i\tau^3_{\beta\alpha}L_{\alpha\beta;\alpha_1\beta_1}\rangle_{\hat{\mathbf{k}}}\Lambda_{\alpha_1\beta_1;\alpha_2\beta_2}\times\langle\hat{\mathbf{k}}_j\tau^3_{\alpha'\beta'}L_{\alpha_2\beta_2;\alpha'\beta'}\rangle_{\hat{\mathbf{k}}}\,, \tag{B3}$$

where we have adopted a shorthand notation suppressing momentum indices in order to better illustrate the particle-hole structure of the problem. The averaged vertices $\langle\hat{\mathbf{k}}L\rangle$ clearly vanish for all even-parity states, as noted in the text. If the order parameter is odd parity, however, we decompose L in Nambu space in the following way:

$$L_{\alpha_1\beta_1,\alpha_2\beta_2}=L_{ij}\tau^i_{\alpha_1\alpha_2}\tau^j_{\beta_2\beta_1}\,, \tag{B4}$$

where now only the components

$$L_{00}\equiv\frac{\Gamma}{\pi}\int d\xi\frac{\tilde{\omega}_+\tilde{\omega}_-}{D},\quad L_{11}=\frac{\Gamma}{\pi}\int d\xi\frac{\Delta_k^2}{D},\quad L_{33}=\frac{\Gamma}{\pi}\int d\xi\frac{\tilde{\xi}_+\tilde{\xi}_-}{D}\,,$$
$$L_{01}=L^*_{10}=\frac{\Gamma}{\pi}\int d\xi\frac{\tilde{\omega}_+\Delta_k}{D},\quad L_{31}=L^*_{13}=\frac{\Gamma}{\pi}\int d\xi\frac{\tilde{\xi}_+\Delta_k}{D} \tag{B5}$$

will be relevant to our analysis. Here we have defined

$$D\equiv(\tilde{\omega}_+^2-\tilde{\xi}_+^2-\Delta_k^2)(\tilde{\omega}_-^2-\tilde{\xi}_-^2-\Delta_k^2) \tag{B5a}$$

and

$$\tilde{\xi}_\pm\equiv\xi_{\mathbf{k}\pm\mathbf{q}/2}+\Sigma_3(\omega\pm i0)\,. \tag{B5b}$$

It is now convenient to find another decomposition of (B2),

$$L_{\alpha_1\beta_1,\alpha_2\beta_2}=\tfrac{1}{2}L^{ij}\tau^i_{\alpha_1\beta_1}\tau^j_{\beta_2\alpha_2}\,, \tag{B6}$$

such that L now acts as a projection operator onto subspace i on the left and j on the right. It is straightforward to show that

$$\begin{aligned}L^{00}&=L_{00}+L_{11}+L_{33}\,,\\ L^{11}&=L_{00}+L_{11}-L_{33}\,,\\ L^{22}&=L_{00}-L_{11}-L_{33}\,,\\ L^{33}&=L_{00}-L_{11}+L_{33}\,,\\ L^{23}&=i(L_{01}-L_{10})=-L^{32}\,,\\ L^{13}&=L_{13}+L_{31}=L^{31}\,,\\ L^{12}&=i(L_{30}-L_{03})=-L^{21}\,.\end{aligned} \tag{B7}$$

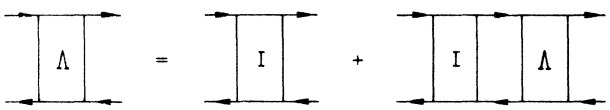

FIG. 9. Integral equations for the vertex function Λ.

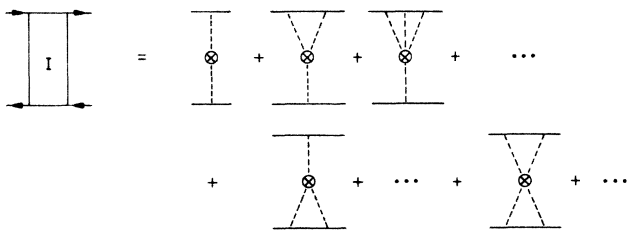

FIG. 10. Diagrams contributing to the irreducible vertex function I.

Inserting (B6) into (B3) and performing all contractions, we find

$$\chi_{Q_iQ_j}=\langle\hat{\mathbf{k}}_i^2 L^{33}\rangle\delta_{ij}+\sum_{n=1,2}\langle\hat{\mathbf{k}}_i L^{3n}\rangle\Lambda_{nm}\langle\hat{\mathbf{k}}_j L^{m3}\rangle\ , \tag{B8}$$

where we have defined

$$\Lambda_{\alpha\beta,\alpha'\beta'}\equiv\tfrac{1}{2}\Lambda_{ij}\tau^i_{\alpha\beta}\tau^j_{\beta'\alpha'}\ . \tag{B9}$$

Thus, calculating χ_{QQ} requires knowledge only of the four components Λ_{11}, Λ_{22}, Λ_{12}, and Λ_{21} of the full vertex function, which obeys the equation depicted schematically in Fig. 9,

$$\Lambda_{\alpha\beta,\alpha'\beta'}=T^+_{\alpha\alpha'}T^-_{\beta'\beta}+T^+_{\alpha\alpha_1}\langle L_{\alpha_1\beta_1,\alpha_2\beta_2}\rangle_{\hat{\mathbf{k}}}T^-_{\beta_1\beta}\Lambda_{\alpha_2\beta_2,\alpha'\beta'}\ . \tag{B10}$$

The equations may be decoupled by using (B6), (B9), and defining

$$I_{ij}\equiv\tfrac{1}{2}\mathrm{Tr}(\underline{\tau}^i\underline{T}^+\underline{\tau}^j\underline{T}^-)\ . \tag{B11}$$

After performing all traces we are left with

$$\Lambda_{ij}=I_{ij}+I_{ii'}\langle L^{i'j'}\rangle_{\hat{\mathbf{k}}}\Lambda_{j'j}\ , \tag{B12}$$

which may be inverted to give

$$\begin{aligned}\Lambda_{11}&=[(1-I_{11}\langle L^{22}\rangle)I_{11}-I_{12}^2\langle L^{22}\rangle]/R\ ,\\ \Lambda_{22}&=[(1-I_{11}\langle L^{11}\rangle)I_{11}-I_{12}^2\langle L^{11}\rangle]/R\ ,\\ \Lambda_{12}&=-\Lambda_{21}=[I_{12}+(I_{12}^2+I_{11}^2)\langle L^{12}\rangle]/R\ ,\end{aligned} \tag{B13}$$

where

$$\begin{aligned}R=&(1-I_{11}\langle L^{22}\rangle+I_{12}\langle L^{12}\rangle)(1-I_{11}\langle L^{11}\rangle+I_{12}\langle L^{12}\rangle)\\&+(I_{11}\langle L^2\rangle+I_{12}\langle L^{22}\rangle)(I_{12}\langle L^{11}\rangle+I_{11}\langle L^{12}\rangle)\ .\end{aligned} \tag{B14}$$

From (B11) we have

$$\begin{aligned}I_{11}&=I_{22}=T_0^+T_0^-T_3^+T_3^-\ ,\\ I_{12}&=i(T_0^+T_3^--T_3^+T_0^-)=-I_{21}\ ,\end{aligned} \tag{B15}$$

which, along with equations (B5), (B7), (B8), (B13), and (B14) completely determine χ_{QQ}. Consideration of the analytic properties of the T matrix and the form of (B15) now make it straightforward to show that the function Λ is both real and even in ω at $\mathbf{q}=\mathbf{0}$. We note that products of two advanced and two retarded Green's functions, which contribute, in principle, to general response functions, vanish identically at $\hat{\mathbf{q}}=\mathbf{0}$, $\Omega=0$ for vertices with symmetry $\hat{\mathbf{k}}_i\underline{\tau}^3\hat{\mathbf{k}}_j\underline{\tau}^3$, as in the present calculation. This is true for both the bare response[37] and vertex corrections.

For completeness, we also give the result for the response function χ_{AA}, where $\underline{A}_k=a(\hat{\mathbf{k}})\underline{\tau}_3$, and the orbital part $a(\hat{\mathbf{k}})$ is even in $\hat{\mathbf{k}}$ (examples are the density and the stress-tensor operators),

$$\begin{aligned}\chi_{AA}=&\langle a(\hat{\mathbf{k}})^2L^{33}\rangle_{\hat{\mathbf{k}}}\\&+\langle a(\hat{\mathbf{k}})L^{33}\rangle_{\hat{\mathbf{k}}}^2\frac{I_{00}^2-I_{03}^2}{I_{00}-(I_{00}^2-I_{03}^2)\langle L^{33}\rangle_{\hat{\mathbf{k}}}}\ .\end{aligned} \tag{B16}$$

Note, however, that the above expression for χ_{AA} is not the complete response function, as pair-interaction-induced vertex corrections are needed to maintain gauge invariance.

*Present address: Department of Applied Physics, Stanford University, Stanford, CA 94305-2184 and Department of Physics, University of California–San Diego, La Jolla, CA 92093.

[1]For reviews, see G. R. Stewart, Rev. Mod. Phys. **56**, 755 (1984); P. A. Lee, T. M. Rice, J. W. Serene, L. J. Sham, and J. W. Wilkins, Comments on Cond. Matt. Phys. **12**, 99 (1986); F. Steglich, in *Theory of Heavy Fermions and Valence Fluctuations,* Vol. 62 of *Springer Series in Solid State Sciences,* edited by T. Kasuya and T. Saso (Springer, Berlin, 1985), p. 23.

[2]H. R. Ott, H. Rudigier, T. M. Rice, K. Ueda, Z. Fisk, and J. L. Smith, Phys. Rev. Lett. **52**, 1915 (1984).

[3]D. J. Bishop, C. M. Varma, B. Batlogg, F. Bucher, Z. Fisk, and J. L. Smith, Phys. Rev. Lett. **53**, 1009 (1984).

[4]D. E. MacLaughlin, Cheng Tien, W. G. Clark, M. D. Lan, Z. Fisk, J. L. Smith, and H. R. Ott, Phys. Rev. Lett. **53**, 1833 (1984).

[5]D. Einzel, P. J. Hirschfeld, F. Gross, B. S. Chandrasekhar, K. Andres, H. R. Ott, J. Bevers, Z. Fisk, and J. L. Smith, Phys. Rev. Lett. **56**, 2513 (1986).

[6]L. Coffey, T. M. Rice, and K. Ueda, J. Phys. C **18**, L813 (1985).

[7]C. J. Pethick and D. Pines, Phys. Rev. Lett. **57**, 118 (1986).

[8]F. Steglich, in Theory of Heavy Fermions and Valence Fluctuations, Ref. 1, p. 23.

[9]R. Felten, F. Steglich, G. Weber, H. Rietschel, F. Gompf, B. Renker, and J. Jeuers, Europhys. Lett. **2**, 323 (1986).

[10]P. Hirschfeld, D. Vollhardt, and P. Wölfle, Solid State Commun. **59**, 111 (1986).

[11]S. Schmitt-Rink, K. Miyake, and C. M. Varma, Phys. Rev. Lett. **57**, (1986).

[12]K. Scharnberg, D. Walker, H. Monien, L. Tewordt, and R. A. Klemm, Solid State Commun. **60**, 535 (1986).

[13]C. M. Varma, Phys. Rev. Lett. **55**, 2723 (1985).

[14]B. Batlogg, D. J. Bishop, B. Golding, E. Bucher, J. Hufnagl, Z. Fisk, J. L. Smith, and H. R. Ott, Phys. Rev. B **33**, 5906 (1986).

[15]P. W. Anderson, Phys. Rev. B **30**, 4000 (1984).

[16]K. Ueda and T. M. Rice, Phys. Rev. B **31**, 7114 (1985).

[17]G. E. Volovik and L. P. Gor'kov, Zh. Eksp. Teor. Phys. **88**, 1412 (1985) [Sov. Phys.—JETP **61**, 843 (1985)].

[18]E. I. Blount, Phys. Rev. B **32**, 2935 (1985).

[19]See, e.g., A. A. Abrikosov, L. P. Gor'kov, and I. E. Dzyaloshinski, *Methods of Quantum Field Theory in Statistical Physics* (Dover, New York, 1963).

[20]J. D. Thompson, M. W. McElfresh, J. O. Willis, Z. Fisk, J. L. Smith, M. B. Maple, Phys. Rev. B **35**, 48 (1987).

[21]P. Hirschfeld, P. Wölfle, and D. Einzel (unpublished).

[22]H. Monien, K. Scharnberg, L. Tewordt, and D. Walker, Solid State Commun. **61**, 581 (1987).

[23]H. Monien, K. Scharnberg, and D. Walker, Solid State Commun. **63**, 263 (1987).

[24]K. Maki, Phys. Rev. **153**, 428 (1967).

[25]H. Shiba, Prog. Theor. Phys. **40**, 435 (1968).
[26]J. Zittartz, A. Bringer, and E. Müller-Hartmann, Solid State Commun. **10**, 513 (1972).
[27]L. J. Buchholtz and G. Zwicknagl, Phys. Rev. B **23**, 5788 (1981).
[28]K. Ueda and T. M. Rice, in *Theory of Heavy Fermions and Valence Fluctuations*, Ref. 1, p. 267.
[29]L. P. Gor'kov and P. A. Kalujin, Pis'ma Zh. Eksp. Teor. Fiz. **41**, 208 (1985) [JETP Lett. **41**, 253 (1985)].
[30]A. A. Abrikosov and L. P. Gor'kov Zh. Eksp. Teor. Phys. **39**, 1781 (1961) [Sov. Phys.—JETP **12**, 1243 (1961)].
[31]A. De Visser, J. C. P. Klaasse, M. van Sprang, J. J. M. Franse, A. Menovsky, and T. T. M. Palstra, J. Magn. Magn. Mater. **54 - 57**, 375 (1986).
[32]H. E. Ott (private communication); G. R. Stewart (private communication).
[33]P. G. de Gennes, *Superconductivity of Metals and Alloys* (Benjamin, New York, 1965).
[34]A. Sulpice, P. Gundit, J. Chaussy, J. Flouquet, D. Jaccard, P. Lejay, and J. L. Tholence, J. Low Temp. Phys. **62**, 39 (1986).
[35]G. R. Stewart, Z. Fisk, J. O. Willis, and J. L. Smith, Phys. Rev. Lett. **52**, 679 (1984).
[36]F. Steglich, U. Rauchschwalbe, U. Gottwick, H. M. Mayer, G. Sparn, N. Grewe, U. Poppe, and J. J. M. Franse, J. Appl. Phys. **57**, 3054 (1985).
[37]V. Ambegaokar and L. Tewordt, Phys. Rev. **134**, A805 (1964).
[38]J. J. M. Franse, A. Menovsky, A. de Visser, C. D. Bredl, U. Gottwick, W. Lieke, H. M. Mayer, U. Rauchschwalbe, G. Sparn, and F. Steglich, Z. Phys. B **59**, 15 (1985).
[39]D. Jaccard and J. Flouquet, J. Magn. Magn. Mater. **47 - 48**, 45 (1985).
[40]N. E. Alekseevskii, A. V. Mitin, A. S. Rudenko, and A. A. Sorokin, Pis'ma Zh. Eksp. Teor. Fiz. **43**, 533 (1986) [JETP Lett. **H3**, 690 (1986)].
[41]K. Maki, in *Superconductivity*, edited by R. D. Parks (Dekker, New York, 1969, p. 1035.
[42]T. Moriya, J. Phys. Soc. Jpn. **18**, 516 (1963).
[43]K. Maki and P. Fulde, Phys. Rev. **140**, A1586 (1965).
[44]H. R. Ott, E. Felder, C. Bruder, and T. M. Rice, Europhys. Lett. **3**, 113 (1987).
[45]L. Taillefer, R. Newbury, G. G. Lonzarich, Z. Fisk, and J. L. Smith, J. Magn. Magn. Mater. **63 - 64**, 372 (1987).
[46]K. Miyake and C. M. Varma, Phys. Rev. Lett. **57**, 1627 (1986).
[47]G. Baym, Phys. Rev. **127**, 1391 (1962).